PHYSICAL PROCESSES AT HIGH FIELD STRENGTHS*

Charles K. Rhodes
Department of Physics, University of Illinois at Chicago
P. O. Box 4348, Chicago, Illinois 60680

CONF-860845--4

DE87 004732

Abstract

The availability of extraordinarily bright femtosecond ultraviolet sources is rapidly extending the study of atomic responses into an unexplored regime for which the electric field strength is considerably in excess of an atomic unit. As this regime is approached, experiments studying multiple ionization, photoelectron spectra, harmonically produced radiation, and fluorescence all exhibit strong nonlinear coupling. Peak total energy transfer rates on the order of ~ 2×10^{-4} W/atom have been observed at an intensity of ~ 10^{16} W/cm^2, and the removal of an electron from an inner principal quantum shell has been demonstrated in xenon. Measurements of the radiation produced by the high field interaction with the rare gases have revealed the presence of both copious harmonic production and fluorescence. The highest harmonic observed was the seventeenth (14.6 nm) in Ne, the shortest wavelength ever produced by that means. Strong fluorescence was seen in Ar, Kr, and Xe with the shortest wavelengths observed being below 10 nm. Furthermore, radiation from inner-shell excited configurations in Xe, specifically the $4d^9 5s5p \rightarrow 4d^{10} 5s$ manifold at ~ 17.7 nm, was detected. The behaviors of the rare gases with respect to multiquantum ionization, harmonic production, and fluorescence were found to be correlated so that the materials fell into two groups, He and Ne in one and Ar, Kr, and Xe in the other. These experimental findings, in alliance with other studies on inner-shell decay processes, give evidence for a role of atomic correlations in a direct nonlinear process of inner-shell excitation. It is expected that an understanding of these high-field processes will enable the generation of stimulated emission in the x-ray range.

MASTER

* Presented at the Vacuum Ultraviolet Radiation Phys. Int. Conf., Aug. 1986, Lund, Sweden. To be published in Physica Scripta.

AC02-83ER13137

DISTRIBUTION OF THIS DOCUMENT IS UNLIMITED

DISCLAIMER

This report was prepared as an account of work sponsored by an agency of the United States Government. Neither the United States Government nor any agency thereof, nor any of their employees, makes any warranty, express or implied, or assumes any legal liability or responsibility for the accuracy, completeness, or usefulness of any information, apparatus, product, or process disclosed, or represents that its use would not infringe privately owned rights. Reference herein to any specific commercial product, process, or service by trade name, trademark, manufacturer, or otherwise does not necessarily constitute or imply its endorsement, recommendation, or favoring by the United States Government or any agency thereof. The views and opinions of authors expressed herein do not necessarily state or reflect those of the United States Government or any agency thereof.

I. Introduction

The availability of an ultraviolet laser technology[1,2] capable of producing subpicosecond pulses with energies approaching the joule level in low divergence beams at high repetition rates has made possible a new regime of physical studies concerning the behavior of matter at extremely high field strengths[3,4]. With this new experimental means, electric field strengths on the order of 100 (e/a_0^2) should be attainable. It is expected that atomic and molecular systems will respond in unusual ways to such strong perturbations. Furthermore, it is believed possible that an understanding of these physical interactions may provide a basis for the generation of stimulated emission in the x-ray range[3] by direct, highly nonlinear coupling of ultraviolet radiation to atoms.

Figure (1) illustrates the parameters of the physical regime, in terms of pulse intensity (I) and pulse time scale (τ), that characterize our experimental studies. It is seen that ultraviolet laser technology[5] will extend the range of physical study a considerable distance into the unexplored area, a zone associated with field strengths far greater than an atomic unit and time scales that are advancing toward an atomic time τ_a. In addition, at the wavelength of 248 nm, intensities above $I_c \sim 5 \times 10^{19}$ W/cm^2 will cause strongly relativistic motions to occur[6].

In recent times, it has been conjectured that fundamentally different atomic motions may be driven under such extreme conditions of irradiation. Indeed, it has been suggested[3,4,7-10] that ordered many-electron motions of outer-shell electrons could lead to enhanced rates of coupling from the radiation field to an atom. In order to study the conditions necessary for

this atomic response to occur and to determine the influence of possible damping mechanisms, the properties of ion charge state distributions[11,12], electron energy spectra[13], and harmonic radiation[14] produced by irradiation of atoms with intense ultraviolet radiation have been previously investigated. In the present discussion, the new experimental results concerning the radiation produced in the nonlinear interaction will be emphasized. Information on earlier studies concerning the ion and electron distributions is thoroughly documented in references [3,4,8,11,12,and 14] and associated citations.

II. Experimental Findings

A. Ion Charge State Spectra

The basic process under study is the collision-free mechanism

$$N\gamma + X \rightarrow X^{q+} + qe^{-}. \qquad (1)$$

In the study of ion production under collision-free conditions[11,14], a recently developed KrF* (248 nm) laser system[2] which produces pulses having a maximal energy of ~ 23 mJ with a pulse duration of ~ 0.5 ps was used. The focusing system used produced a maximum intensity of ~ 10^{16} W/cm^2 at 248 nm in the experimental volume. The ion charge state spectra were determined with a time-of-flight spectrometer after the ions were extracted from the focal volume with a static electric field.

A summary of the overall results for the rare gases[11,12,14] is contained in Table I. As this compilation shows, Ar, Kr, and Xe exhibit comparable maximum charge states and corresponding magnitudes of energy transfer, values which are in marked contrast to the two lighter materials. A change in the behavior, at least in terms of the cross section for energy transfer leading to ionization, appears to occur between Ne and Ar.

In Xe, ionization is observed which involves the removal of an electron from an inner-shell, specifically a shell with a principal quantum number lower than that of the outermost atomic electrons. As illustrated in Fig. (2), this is clearly demonstrated by the detection of Xe^{9+}, an ion that indicates ionization of the 4d-shell. In addition, the xenon spectrum gives an average energy[15] transfer of ~ 130 eV, a value corresponding to an effective average cross section for the nonlinear interaction on the order of $\langle \sigma_{N\gamma} \rangle_{av} \simeq 4 \times 10^{-21}$ cm^2. The observation of Xe^{9+} implies the presence of a peak energy transfer rate on the order of ~ 2×10^{-4} W/atcm.

B. Photoelectron Energy Spectra

Photoelectron energy spectra[4,12-14] for process (1), recorded under collision-free conditions, provide information complementing that given by the measurement of ion charge state distributions. Commonly, the observed electron spectra consist of a characteristic pattern of interwoven above threshold ionization (ATI) ladder line series. As an example, the electron time-of-flight spectra from argon irradiated with a 248 nm, ~ 0.5 ps laser pulse, at different peak intensities, are shown in Fig. (3). At laser intensities too low for the production of higher charge states (e.g. ~ 10^{14} W/cm^2), the principal ATI-ladders leading to the production of Ar^+ in the $^2P^o_{1/2}$ and $^2P^o_{3/2}$ ground multiplet states (which are resolved in the spectra at higher resolution) are readily observed up to the fourth ATI order. At higher laser intensities, new lines appear at ~ 3.5 eV and ~ 4.5 eV together with corresponding higher order features which can be related to the formation of multiply ionized species. A general feature of the electron spectra observed in the rare gases is the appearance of relatively energetic electrons with energies up to a maximum of ~ 250 eV in neon, ~ 200 eV for xenon, and ~ 120 eV for argon.

These were observed in the laser intensity range spanning from 10^{15} W/cm^2 to 10^{16} W/cm^2.

C. Generation of Radiation

The nonlinear interaction, in addition to producing the ions and electrons indicated in reaction (1), can lead to the generation of radiation. In our experiments, we observe the presence of two mechanisms leading to the production of radiation in the extreme ultraviolet range. They are (1) harmonic generation, a parametric scattering process, and (2) the fluorescence of excited states.

The experimental arrangement used to conduct the studies[18] of the radiation produced is illustrated in Fig. (4). A 20 cm (f/10) focal length lens focusses the 248 nm radiation into a target gas supplied by a modified Laser-technics pulsed valve supersonic gas jet. With this optical system, the maximum intensity in the focal region is estimated to be ~ 10^{16} W/cm^2. The gas jet is mounted 10 cm in front of the entrance slit of a 2.2 meter grazing incidence spectrometer (McPherson model 247) equipped with a 600 l/mm gold-coated spherical grating blazed at 120 nm. Radiation produced in the focal volume enters through a 100 μm slit and is dispersed to a position sensitive detector which is mounted tangentially to the Rowland circle of the spectrometer. The resolution and accuracy of the spectrometer-detector system are typically 0.1 nm. The mounting of the detector allows the observation of radiation between 5 nm and 75 nm. The detector consists of a single stage micro-channel plate with a phosphored fiber optic anode. The detection of the photons is achieved by relaying the image of the phosphor screen through a 35 mm Nikon lens to an optical multichannel analyzer. Since the detector could not directly see the 248 nm radiation of the laser, no filter was used to

suppress the background fundamental radiation. Noise subtraction was achieved by determining the background with the gas jet valve closed. The pulsed gas valve, which was modified to allow a backing pressure up to 1000 psi, was typically operated at 600 psi with a pulse repetition rate of 2 Hz. Background pressures in various parts of the apparatus are indicated in Fig. 4. The laser was focused to a position a few hundred microns above the nozzle tip which has a diameter of 0.5 mm and a throat depth of 1 mm. The estimated gas density in the interaction region was ~ 3×10^{18} cm^{-3}.

1. Harmonic Radiation. The scattering mechanism

$$n\gamma(\omega) + X \rightarrow (n\omega) + X \,, \qquad (2)$$

arising from the nonlinear nature of the atomic susceptibility at high field strengths, leads to the generation of harmonic radiation[19]. In the electric dipole approximation for a spatially homogeneous medium, it is well known that n is restricted to odd integers. In these initial studies, all of the rare gases have been used as target materials.

Previously, with radiation at 248 nm in pulses of ~ 15 ps duration, 35.5 nm radiation was produced as the seventh harmonic[20]. In our experiment, conducted at a maximum intensity of ~ 10^{16} W/cm^2, harmonic generation was observed at considerably higher orders, particularly in the lighter materials He and Ne. In addition, it was also found that the signal strength fell rather slowly as the harmonic order increased. For example, in our experiments in He with 248 nm pulses of approximately 1 ps duration, the intensity of the ninth harmonic was approximately a factor of fifty below that of the fifth, a finding that contrasts with the earlier work[20] which showed a decrement of several hundred between adjacent orders. Table II summarizes the maximum harmonic orders and corresponding wavelengths observed in the rare gases.

On the basis of the observed scattering power, it was possible to estimate the cross sections σ_n corresponding to reaction (2). Table III contains the specific values for He and Ne. As an example, the coupling strength shown for the thirteenth harmonic in Ne represents an efficiency of energy conversion of approximately 5×10^{-11}.

Interestingly, the data contained in Table II indicate that a significant change in the harmonic scattering properties occurs between Ne and Ar, the same point at which the energy transfer rates for ionization appeared to change character. Basically, He and Ne, materials with relatively low rates for energy transfer and ionization, generate harmonics copiously, while the opposite relationship holds for the heavier atoms Ar, Kr, and Xe.

The shapes of the spectra of the harmonics for He and Ne suggest a role for multiply excited states in the nonlinear interaction. In both cases, the envelopes of the harmonic spectra exhibit abrupt changes in regions corresponding to energies for which doubly excited levels are known to be present in the neutral atom. In He, this occurs for n = 13 (~ 65 eV), a spectral region rich in doubly excited configurations[21-28]. For Ne, the corresponding position occurs between n = 9 and n = 11, above which doubly excited states have been measured spectroscopically. In addition, it is known that a specific neon doubly excited state, $[2p^4(^3P)3d(^2P)4p\,^1P^o_1$, 442,700±100 $cm^{-1}]$, connected with a dipole allowed transition to the neutral neon ground state exists[29] exactly at the excitation energy (~ 442,800 ± 500 cm^{-1}) corresponding to eleven 248 nm quanta. Such a state could produce a resonant enhancement in the generation of 22.6 nm radiation. Higher multiply excited states could have a similar influence on the production of harmonics for n > 11 in Ne. We note that this spectral region in neon has been recently examined in the study of resonant

enhancement of photoelectron satellites[30].

2. Fluorescence. Electronically excited ions could be produced directly by process (1). Collision-free photoelectron spectra[13] of xenon have explicitly demonstrated the generation of excited electronic levels for both Xe^{2+} and Xe^{3+}, but only of the ground state configuration. In general, if a strong radiative channel is available for decay, a sensitive and selective means for the observation of electronically excited products $(X^{q+})^*$ is by the detection of characteristic radiation. In the current studies, fluorescent emissions from orbitally excited ions of Ar, Kr, and Xe have been observed. A region of the xenon spectrum near the seventh harmonic is illustrated in Fig. (5). No emission of any kind, other than the harmonic lines, was observed in He and Ne.

Table IV summarizes the main properties of the observed fluorescence. In all three cases, a large number of emissions were seen. Although specific identification is often possible, as shown by the examples given in Table IV and Fig. (5), a considerable fraction of the measured transitions cannot be associated with the known spectra of any ionic charge state. It seems possible, particularly in light of the discussion above on the harmonic spectra, that multiply excited levels could account for some of these anomalous spectral features. Presently, the information on the properties of such states, particularly for ionic spectra[45], is quite meager.

From a comparison of the data shown in Table II and Table III we see that the harmonic production and fluorescence are anti-correlated. Specifically, fluorescent emissions are only seen from atoms that are relatively poor generators of harmonic spectra, and the best materials for harmonic generation exhibit no fluorescence. Moreover, the change in the behavior occurs between

Ne and Ar, a division that matches that discussed in relation to the ionization rate. The strong fluorescers are consistently the materials that exhibit high energy transfer rates in the studies of collision-free ionization.

The identified transitions in the spectrum of Xe^{7+}, as shown in Table IV, clearly indicate the presence of two basically different electronic configurations. One involves transitions occurring from excitation of the 5s electron. The other involves excitation of the 4d-shell giving rise to configurations of the form $4d^9 5snp$. This latter result does not come as a complete surprise, since ionization of the 4d-shell was clearly seen in the studies of ion formation. The corresponding 3d excitation in Kr^{7+}, however, has not been identified, although a $3d^9 4p \rightarrow 3d^{10}$ (11.5 nm) transition characteristic of Kr^{8+} appears to be present. We will comment below in Section III on a possible mechanism for excitation of the 4d-shell in xenon.

The currently available data do not unambiguously specify the mechanisms leading to the excitation of the radiating ionic levels. At least three different possibilities exist. They are (a) a direct atomic mechanism which leads to an excited ionic state, (b) recombination, and (c) collisional excitation by energetic electrons in the plasma. For the former, reaction (1) is revised to read

$$N\gamma + X \rightarrow (X^{q+})^* + qe^-, \tag{3}$$

or, if a short-lived intermediate state which autoionizes to the final state is involved, the process can be represented as

$$N\gamma + X \rightarrow (X^{q_1+})^{**} + q_1 e^- \tag{3a}$$

$$\hookrightarrow (X^{q+})^* + (q - q_1)e^- . \tag{3b}$$

In principle, the two paths given by process (3) and reactions (3a) and (3b) are distinguishable for a given $(X^{q+})^*$ level by the distribution of energy among the q electrons that are released. These processes are prompt in the sense that they are generally expected to occur on a subpicosecond time scale.

Recombination[46] and collisional excitation, for the conditions of this experiment, would occur at a much slower rate. For $q \leq 10$, a plasma characterized by a thermal energy of ~ 35 eV, and an electron density $\rho_e \sim 3 \times 10^{18}$ cm^{-3}, the recombination time[47] is approximately 600 ps. Future experiments utilizing an x-ray streak camera will be performed to distinguish these mechanisms.

It is of interest to determine, on the basis of the experimental data, what the equivalent cross section σ_F is assuming that the radiating excited states are generated by the direct processes (3) and (3a)/(3b). This can be accomplished by comparison of the signal for fluorescence to that observed for harmonic generation. Specific cases are given in Table V. Finally, from the comparison of the ion data, which gives a value for energy transfer $\langle\sigma_{N\gamma}\rangle_{av}$, the harmonic data, which establishes σ_n, and the fluorescent emission giving σ_F, we find that the general ordering of these quantities is given by

$$\langle\sigma_{N\gamma}\rangle_{av} > \sigma_F > \sigma_n \qquad (n > 7) \qquad (4)$$

and that

$$\frac{\sigma_F}{\langle\sigma_{N\gamma}\rangle_{av}} \sim 5 \times 10^{-5} \quad . \qquad (5)$$

III. Discussion

The experiments on ion production and on radiation both indicate the excitation and ionization of a 4d electron in xenon. Normally, with irradiation at 248 nm, the 4d inner-electron would be shielded from the external

field[48,49] by the outer 5s and 5p subshells. Therefore, direct coupling of the radiation field to the 4d-shell is not expected to be significant in the neutral atom. Such excitation can occur, however, by an indirect process[9,48]. For xenon, it is well established, particularly from photoionization studies involving multiple-electron ejection[50-55], that the 5p, 5s, and 4d shells exhibit substantial inter-shell coupling[56] and behave in a collective fashion in a manner resembling a single supershell[57]. Some corresponding information on Kr is also available[58].

These intershell couplings provide a basis for the excitation of atomic inner-electrons through radiative interaction with the outer-shell electrons. To explore this point, we consider the single-quantum double-ionization process[53-55] in xenon

$$\gamma + Xe(4d^{10}5s^{2}5p^{6}) \rightarrow Xe^{2+}(4d^{9}5s^{2}5p^{5}) + 2e^{-} \qquad (6)$$

which has an estimated[54] threshold energy of ~ 90 eV. This two-electron process, which represents a significant fraction of the total absorption[54,55], specifically demonstrates the correlated removal of a 5p electron with one from the 4d shell. Therefore, by analogy, this would appear to admit the possibility of nonlinear processes of the type

$$N\gamma + Xe(4d^{10}5s^{2}5p^{6}) \rightarrow Xe^{2+}(4d^{9}5s^{2}5p^{5}) + 2e^{-} \qquad (7)$$

for the neutral atom and corresponding channels of the form

$$N\gamma + Xe^{3+}(4d^{10}5s^{2}5p^{3}) \rightarrow Xe^{5+}(4d^{9}5s^{2}5p^{2}) + 2e^{-} \qquad (8)$$

for ions in which the choice of Xe^{3+} simply serves as an example. In this picture, due to the strong intershell coupling, it should be possible to

produce the same exit channels if sufficient energy is available from the ultraviolet field. In the single-quantum reaction (6) this energy requirement is met by having a frequency sufficiently high so that the quantum energy exceeds the threshold. In the multiquantum process (7) the energy needed is furnished by having an intensity great enough so that the energy of nonlinear coupling to the atom surpasses the threshold value. Processes (6) and (7) are fundamentally similar in the sense that additional channels arise when the main physical parameter governing the reaction, either frequency in the former or intensity in the latter, is sufficiently large. Indeed, since 5s and 5p electrons in such processes are expected to behave similarly[54], a particular possibility is

$$N\gamma + Xe^{5+}(4d^{10}5s^{2}5p) \rightarrow Xe^{7+}(4d^{9}5s5p) + 2e^{-} , \qquad (9)$$

a process that yields the specific excited state generating the 17.7 nm radiation listed in Table V. Therefore, the existence of multielectron processes, which arise as a consequence of the strong intershell coupling, lead naturally, by a nonlinear analogue, to the excitation of the experimentally observed radiating level.

We observe that there is, in principle, no reason to exclude reactions similar to processes (6)-(9) which have greater than two electrons in the final state. Due to the continuous nature of the electron distributions when two or more electrons are produced, however, measurements of photoelectron energy spectra[13] will tend to be insensitive to their presence.

In Section II.C.2, it was stated that the atomic number dependence of (a) the energy transfer for ionization, (b) the harmonic production, and (c) the fluorescence, simultaneously exhibits for these three phenomena a clear

correlation reflecting significant changes in behavior between Ne and Ar. With respect to the comparison of the generation of the harmonic radiation and the fluorescence, a simple graphical picture is presented. Fig. (6a) represents the generation of harmonic radiation. The vertex Σ denotes the classical coupling of the intense incident radiation to the atomic electron, and V is the atomic potential. The nonlinear motion of the driven electron in the atomic potential causes the production of the harmonic radiation. We note that the potential V can be viewed quite generally. It can, for example, arise from a steep gradient in plasma density, a situation corresponding to the circumstances under which strong harmonic production has been observed in plasmas[59]. In cases for which V represents a hard short range potential, high order harmonic radiation is expected.

If the potential V is replaced by a system with internal structure so that excitation becomes possible, we obtain the first piece of Fig. (6b), the inelastic counterpart of Fig. (6a). The second piece of Fig. (6b) denotes fluorescence producing the quantum γ' through the spontaneous transition $B \to C$. Therefore, in Fig. (6a) the energy flows from the incident wave at frequency ω into the harmonic spectra, while in Fig. (6b) the energy flow is channeled into fluorescence through internal excitation of the scattering system. In this picture the internal propagator in the first piece of Fig. (6b) represents the complex intra-atomic couplings discussed above. The diagrams in Fig. (6a) and Fig. (6b) can be readily generalized to the many-electron case. Experimentally, the behavior of He and Ne seems to conform mainly to the process shown in Fig. (6a), while for Ar, Kr, and Xe the response appears to correspond more closely to the mechanism illustrated in Fig. (6b).

IV. Conclusions

The availability of extraordinarily bright femtosecond ultraviolet sources is enabling the study of a wide range of new nonlinear phenomena. Although the exploration of these phenomena is just beginning at relatively low intensities, on the scale of ~ 10^{16} W/cm^2, it has been shown by studies of collision-free ionization that the rate of energy transfer can be extremely high (~ 0.2 mW/atom). Furthermore, the removal of an electron from an inner principal quantum shell in xenon has been demonstrated.

Measurements of the radiation produced by the high field interaction with the rare gases have revealed the presence of both copious harmonic production and fluorescence. All materials produced harmonic radiation and the highest harmonic observed was the seventeenth (14.6 nm) in Ne, the shortest wavelength ever produced by that means. Strong fluorescence was seen only in Ar, Kr, and Xe with the shortest wavelengths observed being below 10 nm. Radiation from inner-shell excited configurations in Xe, specifically, the $4d^9 5s5p \rightarrow 4d^{10} 5s$ manifold at ~ 17.7 nm, was detected.

The behaviors of the rare gases with respect to multiquantum ionization, harmonic production, and fluorescence were found to be correlated so that the materials fell into two groups. The lighter materials He and Ne, although generating high order harmonic radiation, produced no fluorescence and showed significantly weaker coupling for multiphoton ionization. The heavier group, composed of Ar, Kr, and Xe, behaved oppositely. These latter materials are relatively poor producers of harmonic radiation, exhibit strong fluorescence, and are characterized by strong coupling for ionization by multiquantum processes.

The experimental findings of these studies, in combination with other works on inner-shell decay processes, give evidence for a role of atomic correlations in a direct nonlinear process of inner-shell excitation. If such a mechanism is present, it is expected to be a general property of the heavier atoms in the periodic system and, perhaps, a prominent characteristic of actinide species such as uranium. There is the expectation that an understanding of these high-field, nonlinear processes will enable the generation of stimulated emission in the x-ray range.

V. Acknowledgements

The author wishes to acknowledge fruitful discussion with H. Jara, U. Johann, T. S. Luk, I. A. McIntyre, A. McPherson, A. P. Schwarzenbach, M. H. R. Hutchinson, G. Gibson, L. Jönsson, U. Becker, and K. Boyer. The technical assistance of R. Bernico, T. Pack, R. Slagle, and J. Wright is also warmly acknowledged. This work was supported by the U.S. ONR, the U.S. AFOSR, the SDIO(ISTO), the U.S. DOE, the LLNL, the NSF, the DARPA, and the LANL.

VI. References

1. J. H. Glownia, G. Arjavalingham, P. P. Sorokin, and J. E. Rothenberg, Opt. Lett. 11, 79 (1986).

2. A. P. Schwarzenbach, T. S. Luk, I. A. McIntyre, U. Johann, A. McPherson, K. Boyer, and C. K. Rhodes, Opt. Lett. 11, 499 (1986).

3. C. K. Rhodes, Science 229, 1345 (1985).

4. C. K. Rhodes, "Ordered Many-Electron Motions in Atoms and X-Ray Lasers," in Proceedings of the NATO Advanced Study Institute on Giant Resonances in Atoms, Molecules, and Solids, ed. J.-P. Connerade, J. M. Esteva, and R. C. Karnatak (Plenum Press, New York, to be published).

5. Excimer Lasers, 2nd Edition, ed. C. K. Rhodes, (Springer-Verlag, Berlin, 1984).

6. F. V. Bunkin et A. M. Prokhorov in Polarisation, Matiére et Rayonnement, édité par La Société Française de Physique (Presses Universitaires de France, Paris, 1969) p. 157.

7. A. Szöke, J. Phys. B18, L427 (1985).

8. C. K. Rhodes in Multiphoton Processes, P. Lambropoulos and S. J. Smith, editors (Springer-Verlag, Berlin, 1984) p. 31.

9. K. Boyer and C. K. Rhodes, Phys. Rev. Lett. 54, 1490 (1985).

10. A. Szöke and C. K. Rhodes, Phys. Rev. Lett. 56, 720 (1986).

11. T. S. Luk, U. Johann, H. Egger, H. Pummer, and C. K. Rhodes, Phys. Rev. A32, 214 (1985).

12. U. Johann, T. S. Luk, I. A. McIntyre, A. McPherson, A. P. Schwarzenbach, K. Boyer, and C. K. Rhodes, "Multiphoton Ionization in Intense Ultraviolet Laser Fields," in Proceedings of the Topical Meeting on Short Wavelength Coherent Radiation, edited by J. Bokor and D. Attwood (AIP, New York, to be published).

13. U. Johann, T. S. Luk, H. Egger, and C. K. Rhodes, Phys. Rev. A34, 1084 (1986).

14. U. Johann, T. S. Luk, I. A. McIntyre, A. McPherson, A. P. Schwarzenbach, K. Boyer, and C. K. Rhodes, "Multi-Quantum Processes at High Field Strengths," in Proceedings of the Topical Meeting on Short Wavelength Coherent Radiation, ed. J. Bokor and D. Attwood, (AIP, New York, to be published).

15. T. A. Carlson, C. W. Nestor, Jr., N. Wasserman, and J. D. McDowell, Atomic Data 2, 63 (1970).

16. C. E. Moore, Atomic Energy Levels, Vol. I-III, NSRDS-NBS 35 (USGPO, Washington, D.C., 1971).

17. S. Bashkin and J. O. Stoner, Jr., Atomic Energy Level and Grotrian Diagrams Vol. 1-4 and addenda (North-Holland, Amsterdam, 1975-1982).

18. T. S. Luk, A. McPherson, H. Jara, U. Johann, I. A. McIntyre, A. P. Schwarzenbach, K. Boyer, and C. K. Rhodes, "Experimental Study of Harmonic Generation with Picosecond 248 nm Radiation," in Proceedings of the Ultrafast Phenomena Conference (Springer-Verlag, Berlin, to be published).

19. N. Bloembergen, Nonlinear Optics, (W. A. Benjamin, New York, 1965).

20. J. Bokor, P. H. Bucksbaum, and R. R. Freeman, Opt. Lett. 8, 217 (1983).

21. L. Lipsky, R. Anamia, and M. J. Conneely, Atomic Data and Nuclear Data Tables 20, 127 (1977).

22. H. Bachan, J. Phys. B17, 1771 (1984).

23. Y. K. Ho and J. Callaway, J. Phys. B18, 3481 (1985); N. Koyama, H. Fukunda, J. Motoyama, and M. Matsuzawa, J. Phys. B19, L331 (1986).

24. D. H. Oza, J. Phys. B18, L321 (1985).

25. H. Cederquist, M. Kisielinski, and S. Mannervik, J. Phys. B16, L479 (1983).

26. R. Bruch, P. L. Altick, E. Träbert, and P. H. Heckmann, J. Phys. B17, L655 (1984).

27. R. P. Madden and K. Codling, Astrophys. J. 141, 364 (1965).

28. R. P. Madden and K. Codling, Phys. Rev. Lett. 10, 516 (1963).

29. K. Codling, R. P. Madden, and D. L. Ederer, Phys. Rev. 155, 26 (1967).

30. U. Becker, R. Hölzel, H. G. Kerkhoff, B. Langer, D. Szostak, and R. Wehlitz, Phys. Rev. Lett. 56, 1120 (1986).

31. R. L. Kelly and L. J. Palumbo, "Atomic and Ionic Emission Lines Below 2000 Angstroms," NRL Report 7599 (USGPO, Washington, D.C., 1973).

32. R. P. Madden, D. L. Ederer, and K. Codling, Phys. Rev. 177, 136 (1969).

33. A. E. Livingston, L. J. Curtis, R. M. Schectman, and H. G. Berry, Phys. Rev. A21, 771 (1980).

34. K.-T. Cheng and Y.-K. Kim, Atomic Data and Nuclear Data Tables 22, 547 (1978).

35. E. H. Pinnington, W. Ansbacher, and J. A. Kernahan, J. Opt. Soc. Am. B1, 30 (1984).

36. K. Codling and R. P. Madden, Phys. Rev. A4, 2261 (1971).

37. D. L. Ederer, Phys. Rev. A4, 2263 (1971).

38. J. R. Roberts, E. J. Krystautas, and J. Sugar, J. Opt. Soc. Am. 69, 1620 (1979).

39. V. Kaufman and J. Sugar, J. Opt. Soc. Am. B1, 38 (1984).

40. E. J. Krystautas, J. Sugar, and J. R. Roberts, J. Opt. Soc. Am. 69, 1726 (1980).

41. M. Druetta and J. P. Buchet, J. Opt. Soc. Am. 66, 433 (1976).

42. D. J. G. Irwin, J. A. Kernahan, E. H. Pinnington, and A. E. Livingston, J. Opt. Soc. Am. 66, 1396 (1976).

43. J. Blackburn, P. K. Carroll, J. Costello, and G. O'Sullivan, J. Opt. Soc. Am. 73, 1325 (1983).

44. L. J. Curtis and D. G. Ellis, J. Phys. B11, L543 (1978).

45. N. J. Peacock, R. J. Speer, and M. G. Hobby, J. Phys. B2, 798 (1969).

46. D. R. Bates and A. Dalgarno, in Atomic and Molecular Processes, ed. D. R. Bates, (Academic Press, New York, 1962) p. 245.

47. D. R. Bates, A. E. Kingston, and R. W. P. McWhirter, Proc. Roy. Soc. A267, 297 (1962); ibid., A270, 155 (1962).

48. G. Wendin, L. Jönsson, and A. L'Huillier, Phys. Rev. Lett. 56,1241 (1986); A. L'Huillier, L. Jönsson, and G. Wendin, Phys. Rev. A33, 3938 (1986).

49. L. I. Schiff, Phys. Rev. 132, 2194 (1963).

50. M. J. Van der Wiel and T. N Chang, J. Phys. B11, L125 (1978).

51. M. Ya. Amusia, in Advances in Atomic and Molecular Physics, ed. D. R. Bates and B. Bederson, Vol. 17 (Academic Press, New York, 1981) p. 1.

52. S. Southworth, U. Becker, C. M. Truesdale, P. H. Kobrin, D. W. Lindle, S. Owaki, and D. A. Shirley, Phys. Rev. A28, 261 (1983).

53. H. Aksela, A. Aksela, G. M. Bancroft, K. A. Tan, and H. Pulkkinen, Phys. Rev. A33, 3867 (1986).

54. U. Becker, T. Prescher, E. Schmidt, B. Sonntag, and H.-E. Wetzel, Phys. Rev. A33, 3891 (1986).

55. J. Becker, R. Hölzel, H. G. Kerkhoff, B. Langer, D. Szostak, and R. Wehlitz, "Zerfälle der Xe 4d → np Anregungen: resonante Auger - und Doppel-Auger-Prozesse," BESSY Bericht (1984).

56. A. F. Starace, in Fundamental Processes in Energetic Atomic Collisions, ed. H. O. Lutz, J. S. Briggs, H. Kleinpoppen, (Plenum, New York, 1983) p. 69; A. F. Starace, Handb. Physik 31, 1 (1982).

57. M. Ya. Amusia and N. A. Cherepkov, in Case Studies in Atomic Physics 5, ed. E. W. McDaniel and M. R. McDowell (North-Holland, Amsterdam, 1975) p. 47.

58. H. Aksela, S. Aksela, H. Pulkkinen, G. M. Bancroft, and K. H. Tan, Phys. Rev. A33, 3876 (1986).

59. R. L. Carman, C. K. Rhodes, and R. F. Benjamin, Phys. Rev. A24, 2649 (1981).

Table I. Compilation of the maximum ionic charge state q_{max} observed and the corresponding minimum energy transfer required to produce q_{max} for the rare gases under collision-free conditions with irradiation at $\sim 10^{16}$ W/cm^2 with a wavelength of 248 nm and a pulse width of 450 $\pm$ 150 fs. The energy values are derived from the calculated ionization potentials given by Carlson, et. al.[15] and the atomic data tabulated by C. E. Moore[16] and S. Bashkin and J. O. Stoner, Jr.[17]

MATERIAL	MAXIMUM IONIC CHARGE STATE q_{max} OBSERVED	MINIMUM ENERGY TRANSFER TO PRODUCE q_{max} (ev)
He	2	79
Ne	4	224
Ar	8	627
Kr	8	544
Xe	9	630

Table II: Summary of harmonic production observed in the rare gases with 248 nm radiation at an intensity of $\sim 10^{16}$ W/cm^2 and a pulse length of $\sim$ 1 ps.

MATERIAL	MAXIMUM HARMONIC ORDER n	WAVELENGTH OF MAXIMUM HARMONIC (nm)
He	13	19.1
Ne	17	14.6
Ar	7	35.5
Kr	7	35.5
Xe	9	27.6

Table III: Values of harmonic scattering cross sections σ_n for He and Ne observed with 248 nm radiation at an intensity of $\sim 10^{16}$ W/cm^2 and a pulse length of $\sim$ 1 ps.

MATERIAL	HARMONIC SCATTERING CROSS SECTIONS σ_n (cm^2)			
	σ_5	σ_{11}	σ_{13}	σ_{17}
He	$\sim 5 \times 10^{-25}$	$\sim 10^{-28}$	$\sim 5 \times 10^{-29}$	———
Ne	$\sim 2 \times 10^{-24}$	$\sim 2 \times 10^{-28}$	$\sim 2 \times 10^{-28}$	$\sim 7 \times 10^{-29}$

Table IV: Main properties of the fluorescence observed from Ar, Kr, and Xe with 248 nm radiation at an intensity of $\sim 10^{16}$ W/cm^2 and a pulse length of $\sim$ 1 ps.

MATERIAL	ARGON	KRYPTON	XENON
Ionic Charge States Observed	4+, 5+, 6+, 7+	6+, 7+, 8+	6+, 7+, 8+
Wavelength Range of Emissions (nm)	12.0 - 47.1	9.9 - 45.3	9.8 - 48.1
Typical Identified Transitions	$7+$ $4f \rightarrow 3d$	$7+$ $5p \rightarrow 4s$	$7+$ $6s \rightarrow 5p$ ---------- $7+$ $4d^9 5s5p \rightarrow 4d^{10}5s$
Unknown Emissions	Many	Many	Many
References	17,31,32	31,33,34,35,41,42,44	36,37,38,39,40,43

Table V: Tabulation of observed cross sections σ_F for fluorescence assuming that excitation occurs by the direct processes (3) or (3a)/(3b).

MATERIAL	σ_F(cm^2)	SPECIES	TRANSITION	WAVELENGTH (nm)
Kr	$\sim 2 \times 10^{-25}$	Kr^{7+}	$5p \rightarrow 4s$	18.2
Xe	$\sim 2 \times 10^{-25}$	Xe^{7+}	$4d^9 5s5p \rightarrow 4d^{10}5s$	17.7

FIGURE CAPTIONS

Fig. (1): Conditions of irradiation achievable with high brightness subpicosecond ultraviolet sources. Relativistic motions will be prominent above the Compton intensity I_c. The anticipated range of conditions that can be studied is shown in relation to an atomic field strength (E_a) and an atomic time (τ_a).

FIg. (2): Region of the ionic time-of-flight signal recorded at an intensity of ~ 10^{16} W/cm^2 in xenon with 248 nm radiation and a pulse length of 450 $\pm$ 150 fs which specifically illustrates the presence of Xe^{9+}. The peaks in the signals correspond to the distribution of known xenon isotopes.

Fig. (3): Photoelectron time-of-flight spectra for Ar produced at different peak intensities with 248 nm radiation and a pulse length of ~ 0.5 ps.

Fig. (4): Schematic of pulsed gas jet and spectrometer assembly used in studies of emitted radiation.

Fig. (5): Emission spectrum of xenon near the seventh harmonic (354.9 Å) illustrating the characteristic emissions observed with the 248 nm radiation at an intensity of ~ 10^{16} W/cm^2 with a pulse length of ~ 1 ps. In addition to the harmonic line, the 6s + 5p doublet of Xe^{7+}, two lines from the Xe^{6+} 5s6s + 5s5p $^3S_1$ + ^3P_J manifold, and two unidentified features are shown.

Fig. (6): (a) Diagram representing the generation of harmonic radiation.
(b) Diagrams representing the inelastic counterpart of (a) involving the production of excited states and subsequent fluorescence.

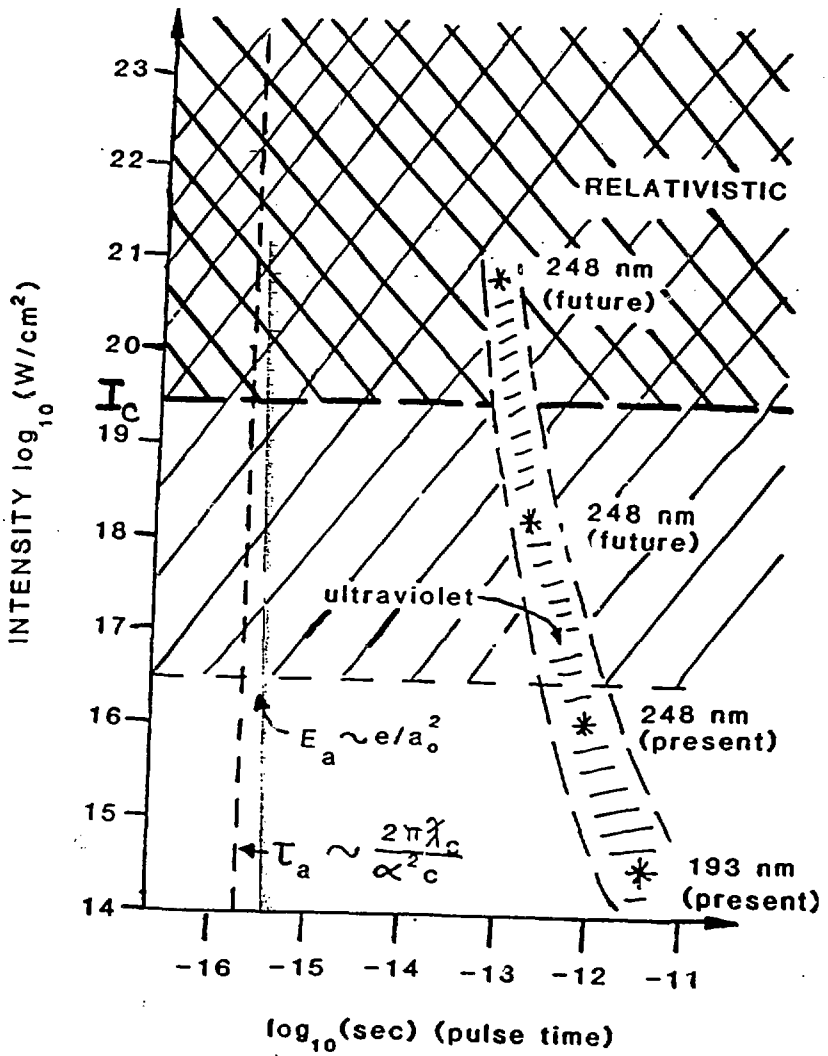
INTENSITY $\log_{10}$ (W/cm^2)
23
22
21
20
19
18
17
16
15
14
I_c
RELATIVISTIC
248 nm (future)
248 nm (future)
ultraviolet
248 nm (present)
193 nm (present)
$E_a \sim e/a_o^2$
$\tau_a \sim \frac{2\pi\lambda_c}{\alpha^2 c}$
-16
-15
-14
-13
-12
-11
$\log_{10}$(sec) (pulse time)

Fig. 1

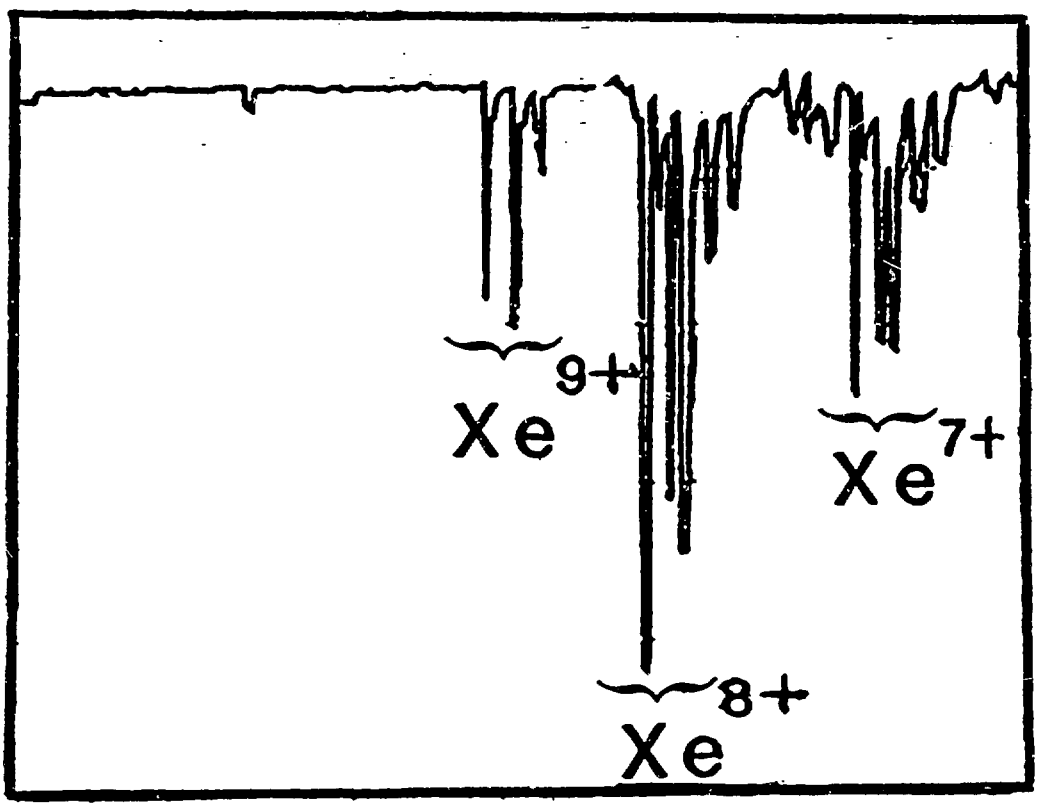

Fig. 2

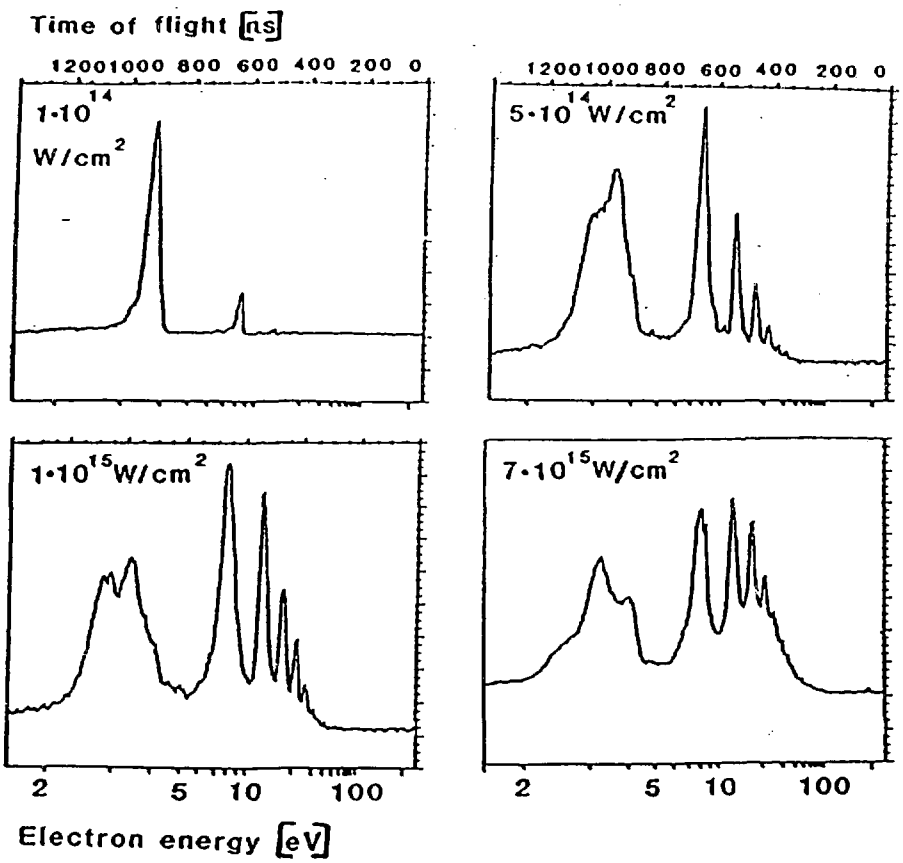
Time of flight [ns]
1200 1000 800 600 400 200 0
1·10^14 W/cm^2
5·10^14 W/cm^2
1·10^15 W/cm^2
7·10^15 W/cm^2
2 5 10 100
Electron energy [eV]

Fig. 3

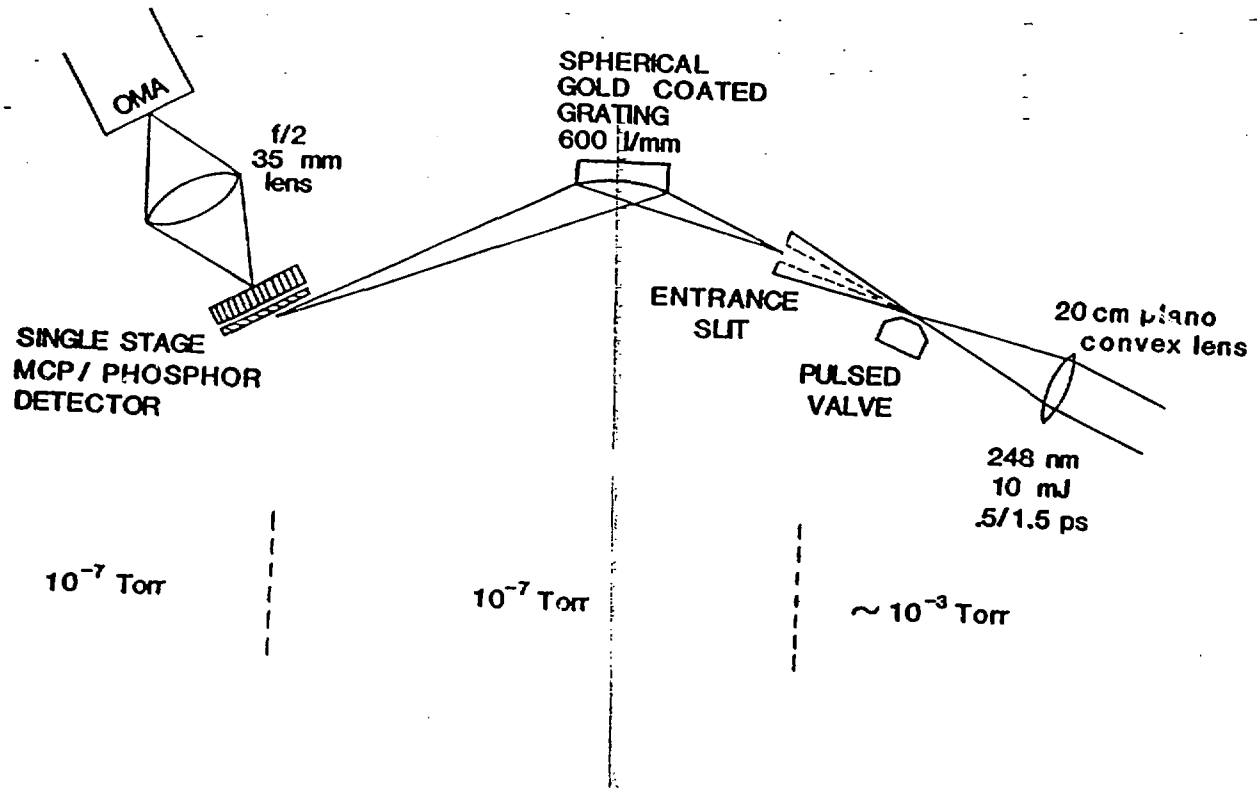
OMA
f/2
35 mm
lens
SPHERICAL
GOLD COATED
GRATING
600 l/mm
SINGLE STAGE
MCP/ PHOSPHOR
DETECTOR
ENTRANCE
SLIT
PULSED
VALVE
20 cm plano
convex lens
248 nm
10 mJ
.5/1.5 ps
10^{-7} Torr
10^{-7} Torr
$\sim 10^{-3}$ Torr

Fig. 4

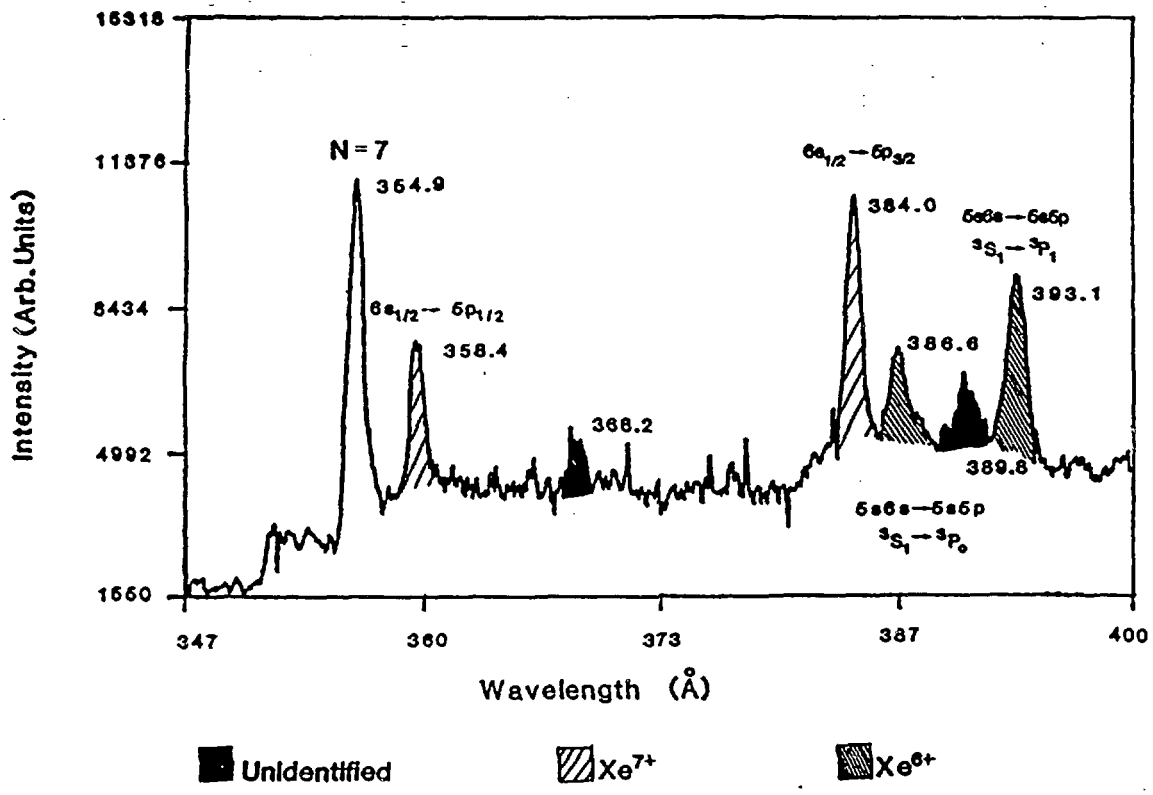
16316
11876
8434
4992
1550
Intensity (Arb. Units)
N = 7
354.9
$6s_{1/2} - 6p_{1/2}$
358.4
366.2
$6s_{1/2} - 6p_{3/2}$
384.0
6s6s—6s6p
$^3S_1 - ^3P_1$
393.1
386.6
389.8
6s6s—6s6p
$^3S_1 - ^3P_0$
347
360
373
387
400
Wavelength (Å)
Unidentified
Xe^{7+}
Xe^{6+}

Fig. 5

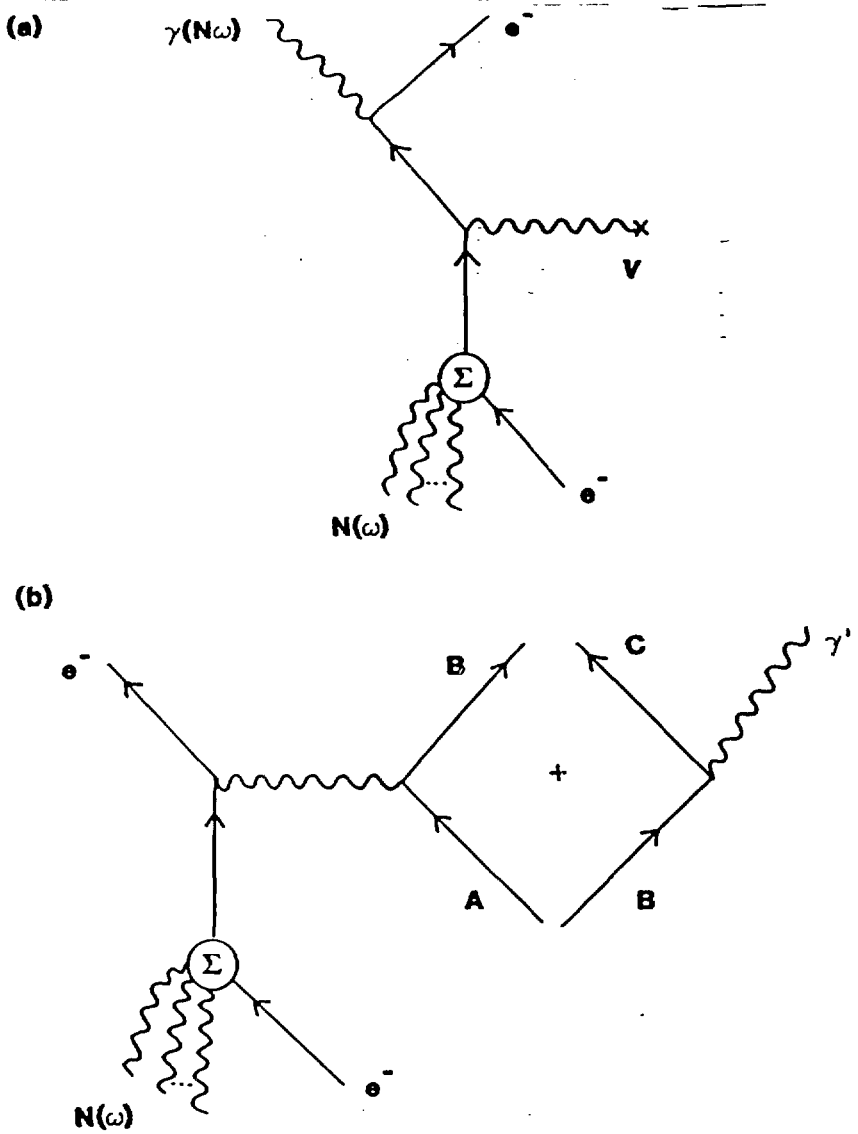

Fig. 6